S1. Technical details on the methodologies for the identification of SI events based on observations (SIO)

In this section, technical details on the SI selection methodologies presented in Sect. 2 are given. These methodologies refer to those used in previous works for NCO-P and Mt. Cimone (see Cristofanelli et al., 2006; Cristofanelli et al., 2010; Cristofanelli et al., 2015).

S1.1 In situ datasets

O_3 and meteorological parameters have been continuously monitored at NCO-P since 2006 and at Mt. Cimone since 1998. Surface O_3 measurements at NCO-P were performed by using a UV-photometric analyser (Thermo Scientific – TEI 49i). The UV-absorption technique was also applied for obtaining O_3 measurements at Mt. Cimone, where a Dasibi 1108 W/GEN was deployed. Since 2006, O_3 measurements at Mt. Cimone were compared every two years against primary standards (reference photometers). These were hosted at the National Institute of Metrological Research (INRiM) in Turin, Italy, in 2006, and at the GAW World Calibration Centre at EMPA (Switzerland) in 2008 and 2010 (here they were compared against the SRP 15 primary standard). Continuous monitoring of ^{7}Be was active at Mt. Cimone between 1998 and 2004, by using a Thermo-Environmental PM_{10} High-Volume sampler (flow rate: 1.13 m^3 min^{-1}) at a time resolution of about 48-h. ^{7}Be concentrations were determined on the sampled glass fiber filters by non-destructive high-resolution g-spectroscopy at 478 keV with HPGe detectors at the Laboratory of Environmental Radiochemistry of the Bologna University (for more details see Tositti et al., 2004). Except for ^{7}Be, all of the other parameters were sampled at 1-min time resolution and aggregated to a common time base of 1 hour. All observations in this paper are expressed in standard temperature and pressure (0 °C and 1013 hPa) and reported at UTC, for avoiding biases when comparing the analyses to the STEFLUX outputs.

S1.2 Total column O_3 retrievals

Concerning NCO-P, the daily total column O_3 (TCO) generated by the NASA Ozone Monitoring Instrument (OMI, Levelt et al., 2006) science team was used. Data referred to the Version-003 of Level-3 Aura/OMI daily global TOMS-Like TCO gridded product (OMTO3e, Bhartia, 2012), calculated on a 1° x 1° pixel encompassing the measurement site location. For Mt. Cimone, daily TCO from the Total Ozone Mapping Spectrometer (TOMS) sensor on board of the NASA "Earth Probe" satellite were considered from 1998 to 2004, while data from the NASA OMI Aura satellite, similarly to those used for NCO-P, were deployed from 2004 to 2010. In this case,

for both datasets the daily overpasses over Sestola (a town sited 7 km NE from Mt. Cimone) were considered.

S1.3 Potential vorticity values

Potential vorticity (PV) values were retrieved by the analysis of back-trajectories reaching both stations. LAGRANTO (Sprenger and Wernli, 2015; Wernli and Davies, 1997) was used as the Lagrangian model to calculate the path of air-masses reaching NCO-P. Its calculations are based on the 6-hourly meteorological 3-D grid composing the operational analysis composed by the ECMWF. A set of 5-day back-trajectories were computed (at 00:00, 06:00, 12:00 and 18:00 UTC); among these, only those centred at an ending altitude of 490 hPa were retained, to minimize possible effects between the model and the real topography. Similarly, PV values were estimated from the 6-day back-trajectories reaching Mt. Cimone, calculated by the FLEXTRA model (Stohl et al., 1995), based again on the analysis field produced by the ECMWF. In this case it has to be noted that, to avoid false detections due to high PV values generated by diabatic processes in the lower troposphere, the PV threshold (see Sect. 1.4 in this Supplementary Material) was applied only for altitudes higher than 5000 m.

S1.4 SI selection criteria

To identify whether a day was likely influenced by SI at NCO-P, at least one of the following four criteria had to be fulfilled:

i. significant variations of daily P values and presence of back-trajectories with values of PV > 1.6 pvu;
ii. significant daily TCO increases and presence of back-trajectories with values of PV > 1.6 pvu;
iii. significant variations of daily P values and significant TCO daily increases;
iv. presence of RH < 60% and significant negative correlation O_3-RH and daily O_3 maximum higher than the seasonal value and significant variation of daily P, PV or TCO values.

Similar criteria were applied to observations at Mt. Cimone, with the addition of ^{7}Be measurements and the relative threshold:

i. significant daily TCO increases and presence of back-trajectories with values of PV > 1.6 pvu;
ii. significant ^{7}Be daily value increases and presence of back-trajectories with values of PV > 1.6 pvu;
iii. presence of RH < 40% and back-trajectories with PV > 1.6 pvu;

iv. RH values lower than 40% and significant TCO daily value increases.

Table S1. Input parameters for STEFLUX for the comparison with in situ measurements (as presented in Sect. 3).

Parameter	NCO-P	Mt. Cimone
Lat_min, Lat_max	26 N, 29 N	43 N, 46 N
Lon_min, Lon_max	85 E, 88 E	9 E, 12 E
Box_top	550 hPa	790 hPa
Time span	01 Mar. 2006 – 31 Dec. 2013	01 Jan. 1998 – 31 Dec. 2010
Temporal resolution	1 h	1 h

Table S2. "SIO vs STEFLUX" and "STEFLUX vs SIO" approaches, as presented in Table 2, for Mt. Cimone, computed by limiting the period of study to 1998 – 2004 (i.e., when data coverage was > 90%).

	"SIO vs STEFLUX"		"STEFLUX vs SIO"	
SI event duration	SI events by SIO	STEFLUX	SI events by STEFLUX	SIO
1 day	115	27 (23%)	61	10 (16%)
2 days	23	9 (39%)	39	15 (38%)
3 days	16	6 (37%)	19	5 (26%)
≥4 days	7	2 (29%)	20	3 (15%)
Total	161	44 (27%)	139	33 (24%)

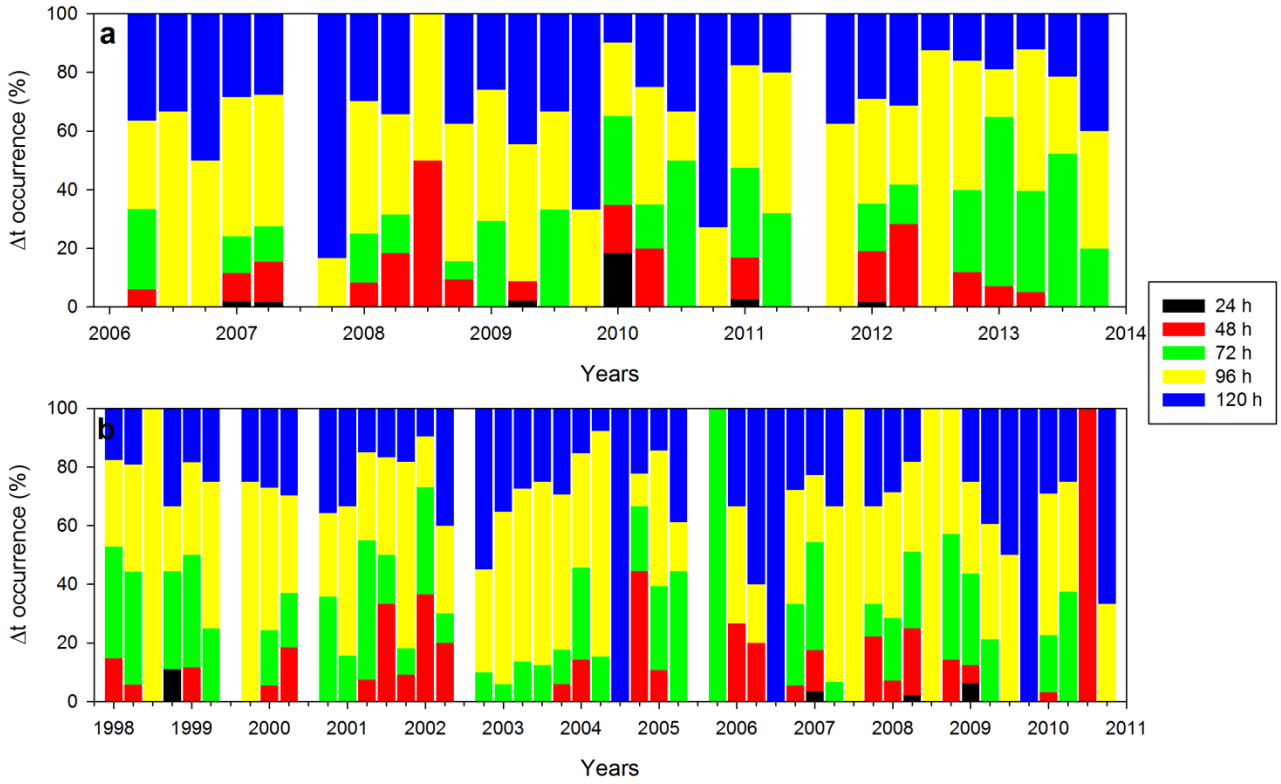

Figure S1. Seasonal graph of Δt occurrence (in %, Δt is defined as the time in hours between the tropopause crossing and the first box crossing) for the SI events identified by STEFLUX (blue line in Fig. 2), for NCO-P (a) and Mt. Cimone (b). Colors in the legend refer to the upper limit of each Δt category, e.g., 24 h refers to 0 h ≤ Δt < 24 h.

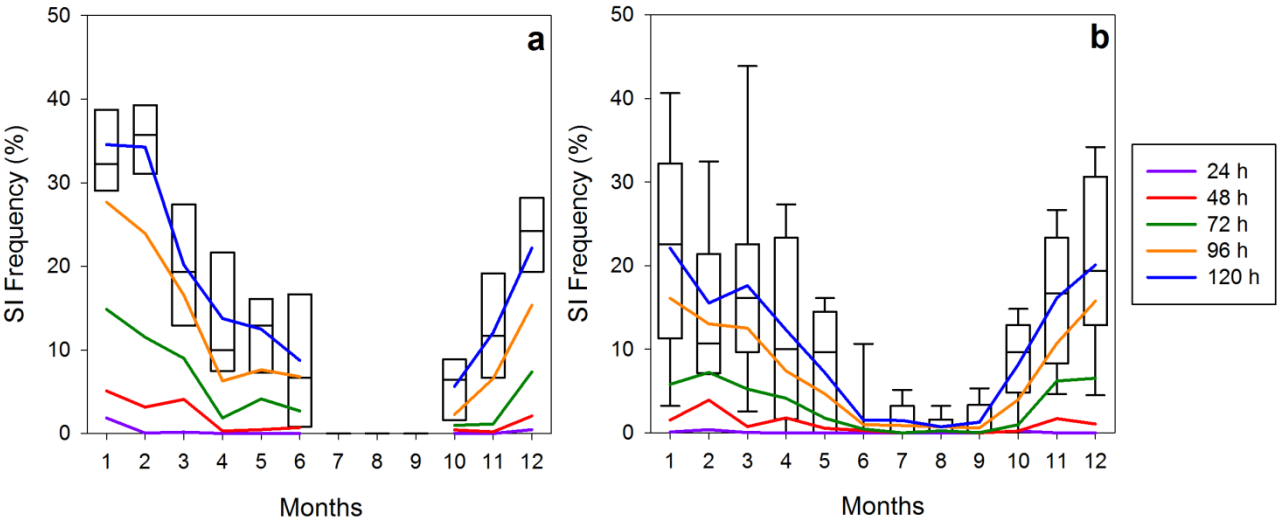

Figure S2. Box-whiskers plot of the annual variation of SI frequency, computed by STEFLUX, at NCO-P (a), and Mt. Cimone (b). Lines define the average monthly contribution from each Δt category. Colors in the legend refer to the upper limit of each Δt category, e.g., 24 h refers to 0 h ≤ Δt < 24 h.

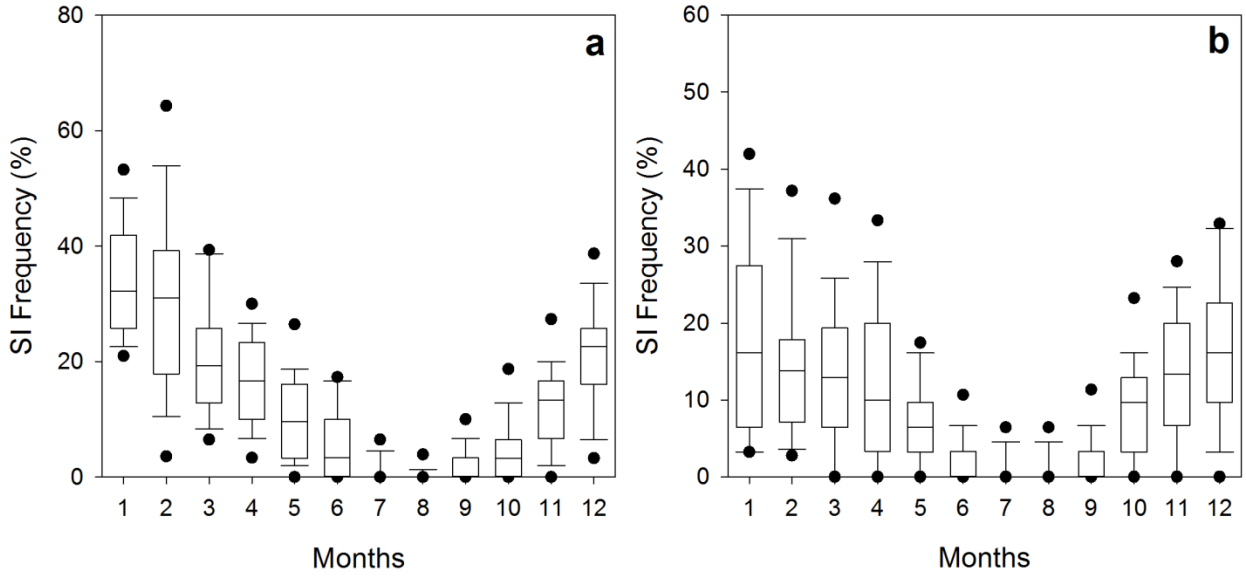

Figure S3. Box-whiskers plot of the annual variation of SI frequency, computed by STEFLUX over the period 1979–2013, for NCO-P (a) and Mt. Cimone (b).

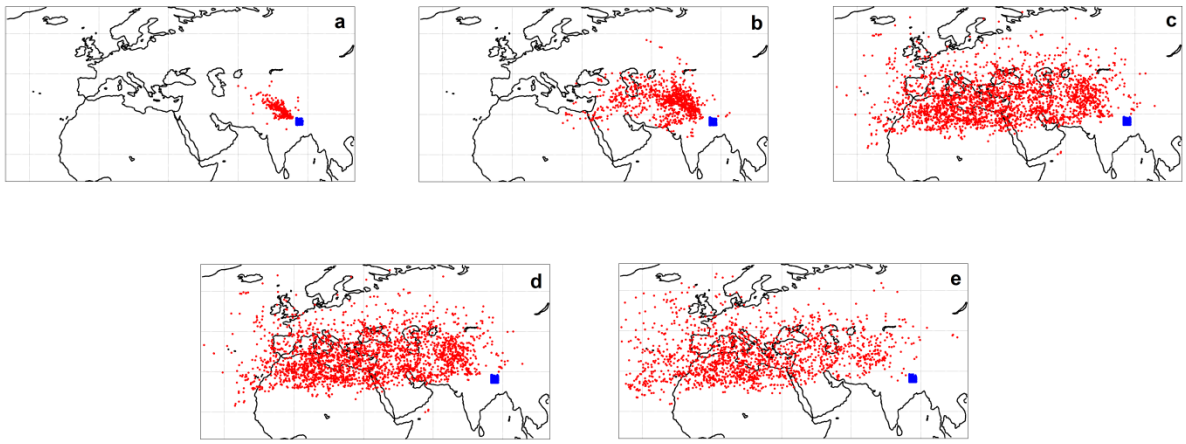

Figure S4. Tropopause crossing (red dots) and first box crossing (blue dots) locations for the SI events at NCO-P over the period 1979–2013. The different panels indicate the Δt categories: 0 h ≤ Δt < 24 h (panel a), 24 h ≤ Δt < 48 h (b), 48 h ≤ Δt < 72 h (c), 72 h ≤ Δt < 96 h (d) and 96 h ≤ Δt < 120 h (e).

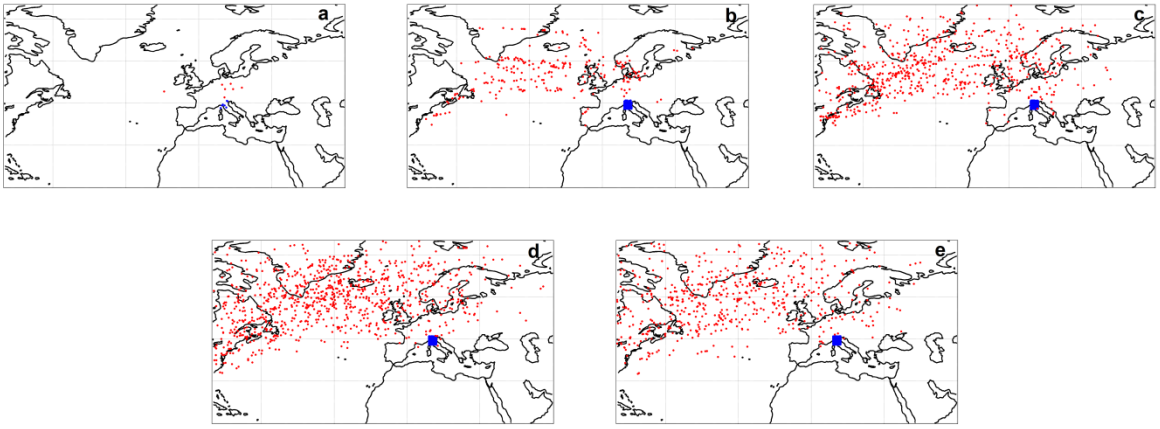

Figure S5. Same as Fig. S4, for Mt. Cimone time series.

References

Bhartia, P. K.: OMI/Aura TOMS-Like ozone, aerosol index, cloud radiance fraction daily L3 Global 1.0x1.0 deg, version 003, NASA Goddard Space Flight Center, doi:10.5067/Aura/OMI/DATA3001.

Cristofanelli, P., Bonasoni, P., Tositti, L., Bonafè, U., Calzolari, F., Evangelisti, F., Sandrini, S., and Stohl, A.: A 6-year analysis of stratospheric intrusions and their influence on ozone at Mt. Cimone (2165m above sea level), J. Geophys. Res., 111, D03306, doi:10.1029/2005JD006553, 2006.

Cristofanelli, P., Bracci, A., Sprenger, M., Marinoni, A., Bonafè, U., Calzolari, F., Duchi, R., Laj, P., Pichon, J.M., Roccato, F., Venzac, H., Vuillermoz, E. and Bonasoni, P.: Tropospheric ozone variations at the Nepal Climate Observatory-Pyramid (Himalayas, 5079 m a.s.l.) and influence of deep stratospheric intrusion events, Atmos. Chem. Phys., 10, 6537-6549, 2010.

Cristofanelli, P., Scheel, H.-E., Steinbacher, M., Saliba, M., Azzopardi, F., Ellul, R., Fröhlich, M., Tositti, L., Brattich, E., Maione, M., Calzolari, F., Duchi, R., Landi, T.C., Marinoni, A., and Bonasoni, P.: Long-term surface ozone variability at Mt. Cimone WMO/GAW global station (2165 m a.s.l., Italy), Atmos. Environ., 101, 23-33, 2015.

Levelt, P. F., van Den Oord, g. H. J., Dobber, M. R. , Malkki, A., Visser, H., de Vries, J., Stammes, P., Lundell, j. O. V., and Saari, H.: The Ozone Monitoring Instrument. IEEE Trans. Geosci. Remote Sens., 44, 1093–1101, doi:10.1109/TGRS.2006.872333, 2006.

Sprenger, M., and Wernli, H.: The Lagrangian analysis tool LAGRANTO – version 2.0, Geosci. Model Dev., 8, 2569-2586, 2015.

Stohl, A., Wotawa, G., Seibert, P., and Kromp-Kolb, H.: Interpolation errors in wind field as a function of spatial and temporal resolution and their impact on different types of kinematic trajectories, J. Appl. Meteorol., 34, 2149-2165, 1995.

Tositti, L., Hübener, S., Kanter, H. J., Ringer, W., Sandrini, S., and Tobler, L.: Intercomparison of sampling and measurement of 7Be in air at four high-altitude locations in Europe, Appl. Radiat. Isotopes, 61, 1497–1502, 2004.

Wernli, H., and Davies, H. C.: A Lagrangian-based analysis of extratropical cyclones. I: The method and some applications, Q. J. Roy. Meteor. Soc., 123, 467-489, 1997.